Modeling Earth Systems and Environment (2023) 9:3517–3526
https://doi.org/10.1007/s40808-022-01664-4

ORIGINAL ARTICLE

Analysis and numerical simulation of a reaction–diffusion mathematical model of atherosclerosis

Debasmita Mukherjee[1] · **Avishek Mukherjee**[2]

Received: 30 September 2022 / Accepted: 23 December 2022 / Published online: 29 January 2023

Abstract
Atherosclerosis is a chronic inflammatory disease which occurs due to plaque accumulation in the intima, the innermost layer of the artery. In this paper, a simple reaction–diffusion mathematical model of the plaque formation process comprising of oxidized LDL and macrophages has been developed. Linear stability analysis of the non-spatial model leads to the existence of global stability of the kinetic system. This reveals that the non-spatial system can withstand a substantial change in the significant model parameter values which can be taken forward for further clinical investigations. Numerical bifurcation analysis of the non-spatial system confirms the existence of Hopf bifurcation with respect to two significant model parameters. The biological importance of these bifurcation diagrams is discussed in detail. The significance of the model presented in this research paper provides a clear insight into the role of the key constituents, oxidized LDL and macrophages, involved in the plaque-forming process.

Keywords Atherosclerosis · Reaction–diffusion system · Global stability · Hopf bifurcation

Mathematics Subject Classification 92B05 · 92C50

Introduction

Atherosclerosis is the leading cause of death in the United States and around the world. The aim of this article is to elucidate the risk factors in atherosclerotic plaque formation in terms of a mathematical model.

According to the 'response to injury' hypothesis atherosclerosis starts with an endothelial lesion (Ross et al. 1977). Damage to the endothelial layer of the artery wall triggers an inflammatory response in which monocytes, T cells, and other immune cells are recruited in the affected area. These cells enter the intima, along with low-density lipoprotein (LDL) and high-density lipoprotein (HDL). In the presence of free oxygen radicals, LDL and HDL particles get oxidized. Monocytes differentiate into macrophages within the intima. Then, macrophages phagocytose oxidized LDL and produce foam cells. The cyclic procedure from monocyte recruitment to foam cell formation continues and it increases the speed of the plaque accumulation process. Eventually, the stress created from the inflated plaque volume crosses the endothelial wall shear stress (WSS) limit. Then, plaque bulges into the lumen and causes hindrance in the smooth blood flow. It results in thrombosis and often leads to serious myocardial infarction (Bulelzai and Dubbeldam 2012).

To understand the complex biological phenomenon of atherosclerotic plaque formation several clinical investigations (Libby et al. 2002; Gijsen et al. 2008; Malek et al. 1999) have been carried out. As the atherosclerotic plaque formation process involves a large number of factors, it is essential to look for computational models to address several queries regarding this pernicious disease. Mathematical models and numerical simulation play a significant role in obtaining better insight into a complex biological phenomenon and subsequently, it helps in generating therapeutic strategies for controlling the disease dynamics. Mathematical models of atherosclerotic plaque formation lead to the ordinary differential equation

✉ Debasmita Mukherjee
debasmita.sarada@gmail.com

Avishek Mukherjee
avishekkgec@gmail.com

[1] Nilkamal School of Mathematics, Applied Statistics and Analytics, SVKM's NMIMS Deemed to be University, Mumbai, India

[2] Tata Consultancy Services, Kolkata, India

(ODE) or partial differential equation (PDE) models. The mathematical models considered to date are able to describe several aspects of the plaque-forming process, for example, cell movement, chemical reactions, coagulation, growth processes, and understanding the complex dynamics of vessel wall (Bulelzai and Dubbeldam 2012; Ougrinovskaia et al. 2010; Cohen et al. 2014; Friedman and Hao 2015; Hao and Friedman 2014; Anlamlert et al. 2017; Alimohammadi 2017; Calvez et al. 2009; Chalmers et al. 2015; Crowther 2005; Cobbold et al. 2002; Ibragimov et al. 2005; Mel'nyk 2019; Abi Younes and El Khatib 2022; Simonetto et al. 2022). An extensive list of mathematical models on atherosclerosis evolution and formation can be found in Parton et al. (2015).

The complexity behind atherosclerotic plaque formation requires a more significant computational model. In this paper, the foremost reason behind atherosclerotic plaque formation, the interaction between oxidized LDL and macrophages has been modeled using a reaction–diffusion system of equations. The plaque formation begins as early as during childhood, then advances in middle age followed by no plaque in the centenarians (Homma et al. 2001). To explain the intricacy of this phenomenon, a logistic growth model is considered in this paper. Michaelis–Menten-type functional response is incorporated for describing the interaction between oxidized LDL and macrophages.

The present article is organized as follows: in "Formulation of the original model", the original model has been formulated. In "Rescaled model" the model has been nondimensionalized. Stability analysis for both the non-spatial and spatial models are performed in "Kinetic system" and "Stability analysis in the presence of diffusion", respectively. Numerical investigations are provided in "Numerical simulation". The discussion of the results is given in "Discussions of the result" followed by concluding remarks in "Concluding remarks".

Formulation of the original model

Macrophage phagocytosis is a significant step in atherosclerotic plaque formation. To analyze the macrophage phagocytosis process a simplified reaction–diffusion model comprising macrophages and oxidized LDL as the dependent variables is presented in this section. An interval $\tilde{\Omega} = [0, \tilde{L}] \subseteq \mathbb{R}$ within the intima is considered in the model description. It is assumed that oxidized LDL and macrophages are diffusing according to Fick's law in $\tilde{\Omega}$. The model is presented as follows:

$$\frac{\partial \tilde{X}}{\partial \tilde{t}} = \phi_1 \tilde{X}\left(1 - \frac{\tilde{X}}{K}\right) - \pi_X \frac{\tilde{M}\tilde{X}}{a\tilde{X} + b\tilde{M}} - \delta_X \tilde{X} + \gamma_1 \tilde{\nabla}^2 \tilde{X}, \quad (2.1)$$

$$\frac{\partial \tilde{M}}{\partial \tilde{t}} = \phi_2 \tilde{M}\left(1 - \frac{c\tilde{M}}{\tilde{X}}\right) - \pi_M \frac{\tilde{M}\tilde{X}}{a\tilde{X} + b\tilde{M}} - \delta_M \tilde{M} + \gamma_2 \tilde{\nabla}^2 \tilde{M}, \quad (2.2)$$

where $\tilde{\nabla}^2 \equiv \frac{\partial^2}{\partial \tilde{x}^2}$. The initial conditions are $\tilde{X}(\tilde{x}, \tilde{t}) > 0, \tilde{M}(\tilde{x}, \tilde{t}) > 0, \forall \tilde{x} \in \tilde{\Omega}$. Here, zero-flux boundary condition $\frac{\partial \tilde{X}}{\partial n} = \frac{\partial \tilde{M}}{\partial n} = 0$ is assumed in $\partial\tilde{\Omega} \times (0, \infty)$, where n is the outward normal vector of the boundary $\partial\tilde{\Omega}$, which is considered to be smooth. Biologically, it means that there is zero movements of macrophages and oxidized LDL outside the region during the numerical observations.

Equations (2.1) and (2.2) represent the respective concentration gradient of oxidized LDL and macrophages, respectively. The genesis of these equations is explained step by step so that we have a complete understanding of the model formulation. Logistic models have been used earlier to describe tumor growth (Kozusko and Bourdeau 2007; Marušić et al. 1994). Here, the macrophage phagocytosis is assumed to follow a logistic growth model. The first terms in Eqs. (2.1) and (2.2) are source terms which are depicting the logistic growth. Intima has a capacity threshold of holding the plaque till it ruptures. The carrying capacity is denoted as K in Eq. (2.1). The concentration of macrophages inside the intima depends on the presence of oxidized LDL. So the source term in Eq. (2.2) is assumed to follow modified logistic growth with carrying capacity directly proportional to the concentration of oxidized LDL. The second terms in Eqs. (2.1) and (2.2) are representing the phagocytosing process of macrophages. The decays of the cellular components are provided in the third terms of the Eqs. (2.1) and (2.2). The last terms in Eqs. (2.1) and (2.2) are depicting the diffusive terms for respective concentration gradients.

Rescaled model

The model in Eqs. (2.1) and (2.2) are rescaled as follows:

The time ($\tilde{t}$) and space ($\tilde{x}$) are changed as:

$$t = \tilde{t}\phi_1, \quad x = \frac{\tilde{x}}{L}.$$

The concentration of oxidized LDL and macrophages are rescaled as the following:

$$X = \tilde{X}/K, \quad M = \tilde{M}/K.$$

Further, all other model parameters are nondimensionalized in the following manner:

$$\lambda_1 = \frac{\pi_X}{\phi_1}, \quad \lambda_2 = \frac{\pi_M}{\phi_1}$$
$$\theta_1 = \frac{\delta_X}{\phi_1}, \quad \theta_2 = \frac{\delta_M}{\phi_1}, \quad \psi = \frac{\phi_2}{\phi_1},$$
$$D_1 = \frac{\gamma_1}{\phi_1 L^2}, \quad D_2 = \frac{\gamma_2}{\phi_1 L^2}.$$

The nondimensionalized model is obtained as follows:

$$\frac{\partial X}{\partial t} = X(1-X) - \lambda_1 \frac{MX}{aX+bM} - \theta_1 X + D_1 \nabla^2 X, \tag{3.1}$$

$$\frac{\partial M}{\partial t} = \psi M\left(1 - \frac{cM}{X}\right) - \lambda_2 \frac{MX}{aX+bM} - \theta_2 M + D_2 \nabla^2 M. \tag{3.2}$$

where

$$\nabla^2 \equiv \frac{\partial^2}{\partial x^2},$$

with the initial condition $X(x,t) > 0,\ M(x,t) > 0, \forall x \in \Omega$, and the boundary condition $\frac{\partial X}{\partial n} = \frac{\partial M}{\partial n} = 0 \in \partial\Omega \times (0,\infty)$.

Kinetic system

To perform the linear stability analysis, first, the kinetic system is considered.

$$\frac{\mathrm{d}X}{\mathrm{d}t} = X(1-X) - \lambda_1 \frac{MX}{aX+bM} - \theta_1 X = H_1(X,M), \tag{4.1}$$

$$\frac{\mathrm{d}M}{\mathrm{d}t} = \psi M\left(1 - \frac{cM}{X}\right) - \lambda_2 \frac{MX}{aX+bM} - \theta_2 M = H_2(X,M). \tag{4.2}$$

with $X(0) > 0, M(0) > 0$.

Stability analysis of the kinetic model

Positivity and boundedness

Theorem *Let all the parameters of the system of Eqs. (4.1), (4.2) be positive and* Γ *be a region in* $\mathbb{R}^2_+$ *defined as,* $\Gamma = \{(X,M) \in \mathbb{R}^2_+ | 0 \le X \le \bar{X}, 0 \le M \le \bar{M}\}$. *Then* Γ *is positive invariant and all the solutions starting from* Γ *are uniformly bounded, the parameters over the bar being the respective upper bounds.*

Proof Clearly, $H_1(X,M)$ and $H_2(X,M)$ are completely continuous and locally Lipchitzian on $C^2(\mathbb{R}^2_+)$. Hence, the solution $(X(t), M(t))$ of (4.1), (4.2) exists and is unique in Γ.

$$\begin{aligned} X(t) =& X(0)\exp\left(\int_0^1 [((1-X(s)) \right. \\ & \left. - \lambda_1 \frac{M(s)}{aX(s)+bM(s)} - \theta_1]\mathrm{d}s\right) \\ \ge& 0, \end{aligned}$$

$$\begin{aligned} M(t) =& M(0)\exp\left(\int_0^1 [\psi(1 - \frac{cM(s)}{X(s)}) \right. \\ & \left. - \lambda_2 \frac{X(s)}{aX(s)+bM(s)} - \theta_2]\mathrm{d}s\right) \\ \ge& 0. \end{aligned}$$

Hence, the positive invariant part is concluded.

Next for the boundedness part, one may observe from (4.1),

$$\frac{\mathrm{d}X}{\mathrm{d}t} \le X(1-X).$$

Then $\lim_{t\to\infty} \sup X(t) \le 1$, as a result of a standard comparison argument. This implies there exists $\mathscr{T} > 0$ such that $X(t) \le N$, for $t > \mathscr{T}$, where $N > 1$. Also from (4.2) , one may observe for $t > \mathscr{T}$,

$$\frac{\mathrm{d}M}{\mathrm{d}t} \le \psi M\left(1 - c\frac{M}{N}\right).$$

Thus, $\lim_{t\to\infty} \sup M(t) \le \frac{N}{c}$. This proves the boundedness of the system (4.1), (4.2).

Equilibrium points and their stability

The equilibrium points of the system (4.1), (4.2) are (i) $E_1 = (X_1, M_1)$ and (ii) $E_2 = (X_2, M_2)$, where $X_1 = 1 - \theta_1$, $M_1 = 0$, $M_2 = \frac{-ac\psi + b\psi - b\theta_2 \pm B}{2bc\psi}$ where $B = \sqrt{a^2c^2\psi^2 + 2abc\psi^2 - 2abc\psi\,\theta_2 + b^2\psi^2 - 2b^2\psi\,\theta_2 + b^2{\theta_2}^2 - 4bc\psi\,\lambda_2}$ and X_2 is a root of the following differential equation ,

$$w_2 z^2 + w_1 z + w_0 = 0,$$

where $w_2 = b^2\lambda_2$, $w_1 = -a^2c\psi\,\lambda_1 - ab\psi\,\lambda_1 + ab\lambda_1\theta_2 + 2b^2\lambda_2\theta_1 - 2b^2\lambda_2 + 2b\lambda_2\lambda_1$, $w_0 = -a^2c\psi\,\lambda_1\theta_1 + a^2c\psi\,\lambda_1 - ab\psi\,\lambda_1\theta_1 + ab\lambda_1\theta_2\theta_1 + b^2\lambda_2{\theta_1}^2 + ab\psi\,\lambda_1 - ab\lambda_1\theta_2 - a\psi\,{\lambda_1}^2 + a{\lambda_1}^2\theta_2 - 2b^2\lambda_2\theta_1 + 2b\lambda_2\lambda_1\theta_1 + b^2\lambda_2 - 2b\lambda_2\lambda_1 + \lambda_2{\lambda_1}^2$.

The Jacobian matrix of the system (4.1), (4.2) is

$$J = \begin{bmatrix} 1 - 2X - \frac{\lambda_1 M^2 b}{(bM+Xa)^2} - \theta_1 & -\frac{\lambda_1 X^2 a}{(bM+Xa)^2} \\ \frac{\psi M^2 c}{X^2} - \frac{\lambda_2 M^2 b}{(bM+Xa)^2} & \frac{-2\psi Mc + X\psi}{X} - \frac{\lambda_2 X^2 a}{(bM+Xa)^2} - \theta_2 \end{bmatrix}. \tag{4.3}$$

The Jacobian evaluated at $E_i, i = 1, 2$ are denoted as as $J_k, k = 1, 2$.

Theorem *The system* (4.1), (4.2) *is locally asymptotically stable at* E_1 *if the following conditions are satisfied*

$$(i)\ \theta_1 < 1 \text{ and } (ii)\ \psi < \frac{\lambda_2}{a} - \theta_2\,.$$

Proof The Jacobian matrix of the system (4.1), (4.2) at E_1 is obtained as the following

$$J_1 = \begin{bmatrix} -1+\theta_1 & -\frac{\lambda_1}{a} \\ 0 & \psi - \frac{\lambda_2}{a} + \theta_2 \end{bmatrix}.$$

Now, the eigenvalues of J_1 are $\upsilon_1 = -1 + \theta_1$ and $\upsilon_2 = \psi - \frac{\lambda_2}{a} - \theta_2$. Thus whenever $\upsilon_1 < 0$ and $\upsilon_2 < 0$, the system (4.1), (4.2) is locally asymptotically stable at E_1, otherwise it is unstable. Then, it is clear that $\upsilon_1 < 0$ whenever $\theta_1 < 1$. Also, if $\psi < \frac{\lambda_2}{a} + \theta_2$ holds, then one may have $\lambda_2 < 0$. Thus, the conditions for the system (4.1), (4.2) to be locally asymptotically stable are: (i) $\theta_1 < 1$ and (ii) $\psi < \frac{\lambda_2}{a} + \theta_2$. It completes the proof.

Theorem *The system* (4.1), (4.2) *is locally asymptotically stable at* E_2 *if and only if* $(i)\ Tr(J_2) < 0$ *and* $(ii)\ det(J_2) > 0$.

Proof The Jacobian matrix of (4.1), (4.2) at E_2 is

$$J_2 = \begin{bmatrix} 1 - 2X_2 - \frac{\lambda_1 {M_2}^2 b}{(aX_2+bM_2)^2} - \theta_1 & -\frac{\lambda_1 {X_2}^2 a}{(aX_2+bM_2)^2} \\ \frac{\psi {M_2}^2 c}{{X_2}^2} - \frac{\lambda_2 {M_2}^2 b}{(aX_2+bM_2)^2} & \frac{-2c\psi M_2 + \psi X_2}{X_2} - \frac{\lambda_2 {X_2}^2 a}{(aX_2+bM_2)^2} - \theta_2 \end{bmatrix} = \begin{bmatrix} \Gamma_{11} & \Gamma_{12} \\ \Gamma_{21} & \Gamma_{22} \end{bmatrix}. \tag{4.4}$$

The characteristic equation of J_2 is $z^2 + K_1 z + K_2 = 0$, where $K_1 = -(\Gamma_{11} + \Gamma_{22})$ and $K_2 = \Gamma_{11}\Gamma_{22} - \Gamma_{12}\Gamma_{21}$. The system (4.1), (4.2) is locally asymptotically stable at E_2 if and only if the Jacobian matrix J_2 has negative eigenvalues. Applying Routh Hurwitz criterion on the second-order polynomial $z^2 + K_1 z + K_2 = 0$, one may conclude that the matrix J_2 has negative eigenvalues if and only if $K_1 > 0$ and $K_2 > 0$. This implies, the system (4.1), (4.2) is locally asymptotically stable at E_2 if and only if (i) $(\Gamma_{11} + \Gamma_{22}) = Tr(J_2) < 0$ and (ii) $\Gamma_{11}\Gamma_{22} - \Gamma_{12}\Gamma_{21} = det(J_2) > 0$. This completes the proof.

Theorem *The model* (4.1), (4.2) *is globally stable at* E_2 *if the following conditions are satisfied:*

$$\max(\Xi_{12} + \Xi_{22}) \le \min(\Xi_{11} + \Xi_{21}),$$

where $\Xi_{ij}, i, j = 1, 2$ *are provided in the proof.*

Proof Consider

$$V = \left(X - X_2 - X_2 ln\frac{X}{X_2}\right) + \left(M - M_2 - M_2 ln\frac{M}{M_2}\right) = \sum_{i=1}^{2} \Xi_i, \tag{4.5}$$

where $\Xi_i = \left(g_i - g_{i_2} - g_{i_2} ln\frac{g_i}{g_{i_2}}\right)$ and $g_i = X, M$ for $i = 1, 2$, respectively.

Now at E_2 the right hand sides of Eqs. (4.1), (4.2) is 0 and hence we obtain,

$$\theta_1 = (1 - X_2) - \lambda_1 \frac{M_2}{aX_2 + bM_2}, \tag{4.6}$$

$$\theta_2 = \psi\left(1 - \frac{cM_2}{X_2}\right) - \lambda_2 \frac{X_2}{aX_2 + bM_2}. \tag{4.7}$$

Then, a straightforward calculation implies the following:

$$\dot{V} = \sum_{i=1}^{2} \dot{\Xi}_i = \sum_{i=1}^{2} \left(1 - \frac{g_{i_2}}{g_i}\right)\dot{g}_i, \tag{4.8}$$

where

$$\dot{\Xi}_1 \le -\Xi_{11} + \Xi_{12},$$
$$\dot{\Xi}_2 \le -\Xi_{21} + \Xi_{22},$$

and

$$\Xi_{11} = (X - X_2)^2,$$
$$\Xi_{12} = \lambda_1 a(M_2 X^2 + X_2^2 M),$$
$$\Xi_{21} = -\frac{c\psi}{X_2}(M - M_2)^2$$
$$\Xi_{22} = c\psi(M_2 X_2 + MX)M + \lambda_2[aX_2(M_2 + M)X + b(X_2 M^2 + XM_2^2)].$$

Thus, if

$$\max(\Xi_{12} + \Xi_{22}) \le \min(\Xi_{11} + \Xi_{21}), \tag{4.9}$$

then one may conclude that,

$$\dot{V} \le 0. \tag{4.10}$$

Also from Eq. (4.8), it is clear that $\dot{V} = 0$ at E_2. Therefore, using Lyapunov–Lasalle's invariance principle (Hale 1969), the proof is concluded.

Bifurcation analysis

Theorem *The model* (4.1), (4.2) *has a Hopf bifurcation around* E_2 *at* $\lambda_1 = \lambda_{1_{[HB]}}$, *where* $\lambda_{1_{[HB]}} = \frac{T}{X_2 {M_2}^2 b}$, *and*

$$T = a^2 {X_2}^3 + 2abM_2 {X_2}^2 - a{X_2}^3\lambda_2 + b^2 {M_2}^2 X_2 - 2a^2 c\psi M_2 {X_2}^2 - 4abc\psi {M_2}^2 X_2 - 2b^2 c\psi {M_2}^3 - a^2\psi {X_2}^3 - 2a^2 {X_2}^4 - a^2 {X_2}^3\theta_1 - a^2 {X_2}^3\theta_2 - 2ab\psi M_2 {X_2}^2 - 4abM_2 {X_2}^3 - 2abM_2 {X_2}^2\theta_1 - 2abM_2 {X_2}^2\theta_2 - b^2\psi {M_2}^2 X_2 - 2b^2 {M_2}^2 {X_2}^2 - b^2 {M_2}^2 X_2\theta_1 - b^2 {M_2}^2 X_2\theta_2.$$

Proof The Hopf bifurcation of the system (4.1), (4.2) occurs if and only if there exists a critical value of λ_1, i.e, $\lambda_1 = \lambda_{1_{[HB]}}$, such that

(i) $\mathrm{tr}(J_2) = \Gamma_{11} + \Gamma_{22} = 0$ at $\lambda_1 = \lambda_{1_{[HB]}}$;
(ii) $\det(J_2) = \Gamma_{11}\Gamma_{22} - \Gamma_{12}\Gamma_{21} > 0$ at $\lambda_1 = \lambda_{1_{[HB]}}$;
(iii) the characteristic equation is $h^2 + \det(J_2) = 0$ at $\lambda_1 = \lambda_{1_{[HB]}}$, whose eigenvalues are purely imaginary;
(iv) $\frac{\mathrm{d}h_1}{\mathrm{d}\lambda_1}|_{\lambda_1 = \lambda_{1_{[HB]}}} \neq 0$, where the eigenvalues of the linearized system about the equilibrium point J_2 is $h_1 \pm ih_2$.

After replacing h by $h = h_1 + ih_2$ in $h^2 - \mathrm{tr}(J_2)h + \det(J_2) = 0$ and separating the real and imaginary parts, one can have

$$(h_1^2 - h_2^2) - tr(J_2) + \det(J_2) = 0, \tag{4.11}$$

$$2h_1h_2 - \mathrm{tr}(J_2)h_2 = 0. \tag{4.12}$$

Next differentiating (4.12) with respect to λ_1, one gets,

$$\frac{\mathrm{d}h_1}{\mathrm{d}\lambda_1}|[\lambda_1 = \lambda_{1_{[HB]}}] = -\frac{{M_2}^2 b}{\left(aX_2 + bM_2\right)^2} \neq 0.$$

The above condition is called the transversality condition. The transversality condition states that in the case of Hopf bifurcation the eigenvalues cross the imaginary axis with non-zero speed. Therefore, the system (4.1), (4.2) observes a Hopf bifurcation around E_2 at $\lambda_1 = \lambda_{1_{[HB]}}$, where

$$\lambda_{1_{[HB]}} = \frac{T}{X_2 {M_2}^2 b}, \quad \text{and} \quad T = a^2 {X_2}^3 + 2abM_2 {X_2}^2 - a{X_2}^3\lambda_2 + b^2 {M_2}^2 X_2 - 2a^2 c\psi M_2 {X_2}^2 - 4abc\psi {M_2}^2 X_2 - 2b^2 c\psi {M_2}^3 - a^2\psi {X_2}^3 - 2a^2 {X_2}^4 - a^2 {X_2}^3\theta_1 - a^2 {X_2}^3\theta_2 - 2ab\psi M_2 {X_2}^2 - 4abM_2 {X_2}^3 - 2abM_2 {X_2}^2\theta_1 - 2abM_2 {X_2}^2\theta_2 - b^2\psi {M_2}^2 X_2 - 2b^2 {M_2}^2 {X_2}^2 - b^2 {M_2}^2 X_2\theta_1 - b^2 {M_2}^2 X_2\theta_2.$$

Stability analysis in the presence of diffusion

The local stability analysis of the spatial system (3.1), (3.2) is analyzed in this section. The self-diffusion coefficients of oxidized LDL and macrophages are denoted as D_1 and D_2, respectively. The linearized system corresponding to (3.1), (3.2) about the non-zero equilibrium $E_2(X_2, M_2)$ is:

$$\frac{\partial \mathscr{X}}{\partial t} = \Gamma_{11}\mathscr{X} + \Gamma_{12}\mathscr{M} + D_1\nabla^2\mathscr{X}, \tag{5.1}$$

$$\frac{\partial \mathscr{M}}{\partial t} = \Gamma_{21}\mathscr{X} + \Gamma_{22}\mathscr{M} + D_2\nabla^2\mathscr{M}, \tag{5.2}$$

where $X = X_2 + \mathscr{X}$, $M = M_2 + \mathscr{M}$. The details of Γ_{ij} can be found in (4.4) for $i, j = 1, 2$. Here, $(\mathscr{X}, \mathscr{M})$ are the small perturbations of (X, M) about the equilibrium point $E_2(X_2, M_2)$. One may assume

$$\begin{bmatrix}\mathscr{X}\\ \mathscr{M}\end{bmatrix} = \begin{bmatrix}v_1\\ v_2\end{bmatrix} e^{\lambda t + ikx},$$

where $\lambda > 0$, $v_i > 0$ represent the amplitude $(i = 1, 2)$ and k is the wave number of the perturbation in time t. The system (5.1), (5.2) becomes,

$$\frac{\partial \mathscr{X}}{\partial t} = (\Gamma_{11} - D_1k^2)\mathscr{X} + \Gamma_{12}\mathscr{M}, \tag{5.3}$$

$$\frac{\partial \mathscr{M}}{\partial t} = \Gamma_{21}\mathscr{X} + (\Gamma_{22} - D_2k^2)\mathscr{M}. \tag{5.4}$$

At $E_2(X_2, M_2)$ the characteristic equation of the linearized system (5.3), (5.4) can be written as:

$$\mu^2 + \hat{K}_1\mu + \hat{K}_2 = 0,$$

where $\hat{K}_1 = K_1 + (D_1 + D_2)k^2$ and $\hat{K}_2 = K_2 - (D_1\Gamma_{22} + D_2\Gamma_{11})k^2 + D_1D_2k^4$.

Theorem *The diffusive system* (3.1), (3.2) *is stable whenever* $D_1\Gamma_{22} + D_2\Gamma_{11} < 0$.

Proof Using Routh–Hurwitz criterion on the second-order polynomial $\mu^2 + \hat{K}_1\mu + \hat{K}_2 = 0$, one may observe that the spatial system (3.1), (3.2) is stable at the positive equilibrium point $E_2(X_2, M_2)$ whenever $\hat{K}_1 > 0$ and $\hat{K}_2 > 0$. One already has obtained $K_1 > 0$ and $K_2 > 0$ as the stability criterion for the kinetic system (4.1), (4.2). It is clear from the definition of $\hat{K}_1$ that $\hat{K}_1 > 0$. Now suppose $\hat{K}_2 = K_2 - \upsilon_1k^2 + \upsilon_2k^4$, where $\upsilon_1 = D_1\Gamma_{22} + D_2\Gamma_{11}$ and $\upsilon_2 = D_1D_2$. Then, it is obvious that $\upsilon_2 > 0$. Thus if $D_1\Gamma_{22} + D_2\Gamma_{11} < 0$, then $\upsilon_1 < 0$.

Then, the required condition $\hat{K}_2 > 0$ follows. Hence, the proof is completed.

Theorem *The condition for diffusive-driven instability of the system* (3.1), (3.2) *at* $E_2(X_2, M_2)$ *is given by,* $K_2 + \upsilon_2 k^4 < \upsilon_1 k^2$, *i.e if* $K_2 + k^4 D_1 D_2 < (D_1\Gamma_{22} + D_2\Gamma_{11})k^2$.

Proof From the above Theorem 5, it is clear that $\hat{K}_1 > 0$ is always under the stability condition of the non-spatial system. The instability part of the spatial system is dependent on the sign of $\hat{K}_2$. So if $\hat{K}_2 < 0$, the diffusive system becomes unstable. The condition $\hat{K}_2 < 0$ is implied by $K_2 + \upsilon_2 k^4 < \upsilon_1 k^2$ or $K_2 + k^4 D_1 D_2 < (D_1\Gamma_{22} + D_2\Gamma_{11})k^2$. So whenever, $K_2 + k^4 D_1 D_2 < (D_1\Gamma_{22} + D_2\Gamma_{11})k^2$ one has $\hat{K}_2 < 0$. This completes the proof.

Table 1 List of parameter values used in the model

Parameters	Non-dimensionalized numeric values
λ_1	0.22
a	0.1
b	0.2
θ_1	0.1
ψ	0.2
c	0.7
λ_2	0.001
θ_2	0.025

Numerical simulation

The numerical simulation results for both the spatial (3.1), (3.2) and non-spatial (4.1), (4.2) systems with respect to the parameter values in Table 1 are discussed in this section.

The equilibrium points of the kinetic model (4.1), (4.2) are obtained as $E_1 = (0.90, M = 0)$, $E_2 = (X = 0.1180, M = 0.1450)$, here E_1 is the boundary equilibrium and E_2 is the positive equilibrium point. The eigenvalues of the Jacobian matrix J_1 are $(-0.9, 0.1650)$ and that of J_2 are $(-0.0308 \pm i0.1382)$. This implies that the kinetic system (4.1), (4.2) is unstable at the boundary equilibrium point E_1 and is stable at the positive equilibrium point E_2. The nullclines of the non-spatial system (4.1), (4.2) based on the model parameter values provided in Table 1 is provided in Fig. 1. The stability attributes of the positive equilibrium point E_2 for both the non-spatial and spatial atherosclerotic models are described in Fig. 2a, b, respectively, based on model parameter values provided in Table 1.

Figure 3 is representing the Hopf bifurcation in the kinetic model with respect to the model parameter λ_1. The phase portrait of the kinetic model (4.1), (4.2) keeping $\lambda_1 = 0.233$ and the rest of the parameter values same as in Table 1 is provided in Fig. 3a. In the spatial counterpart under the same set of parameter values of Fig. 3a one may observe an oscillatory behavior in the oxidized LDL and macrophage concentration in Fig. 3b.

Figure 4 is depicting another Hopf bifurcation in the kinetic model with respect to the model parameter a. The phase portrait with $a = 0.06$ while keeping all other

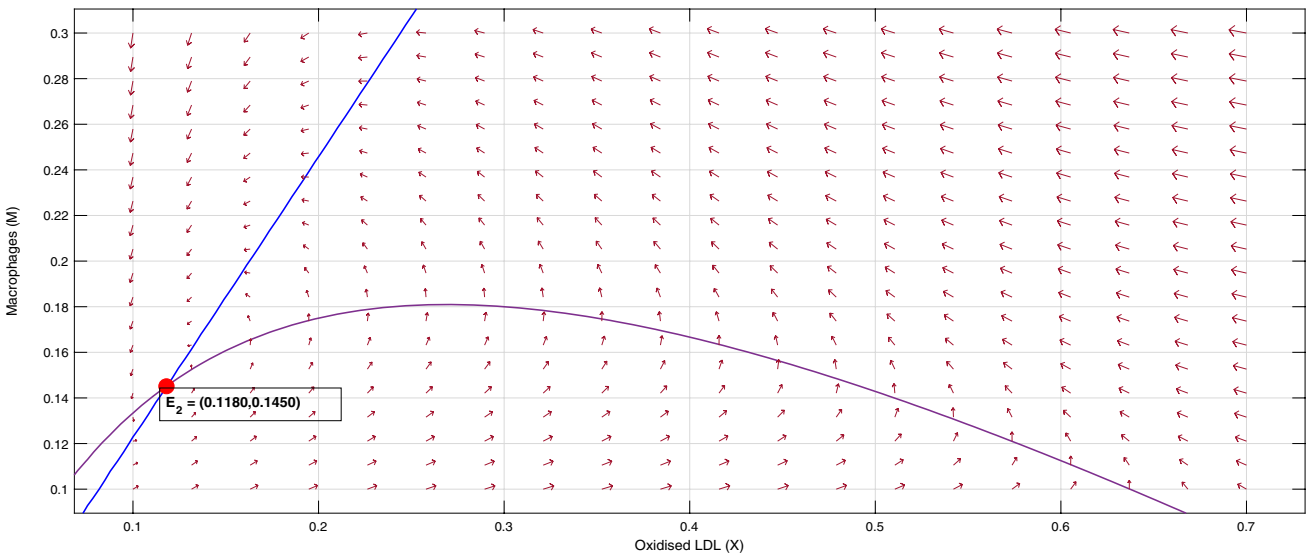

Fig. 1 Nullclines of the non-spatial system (4.1), (4.2) with all the model parameter values are same as provided in Table 1

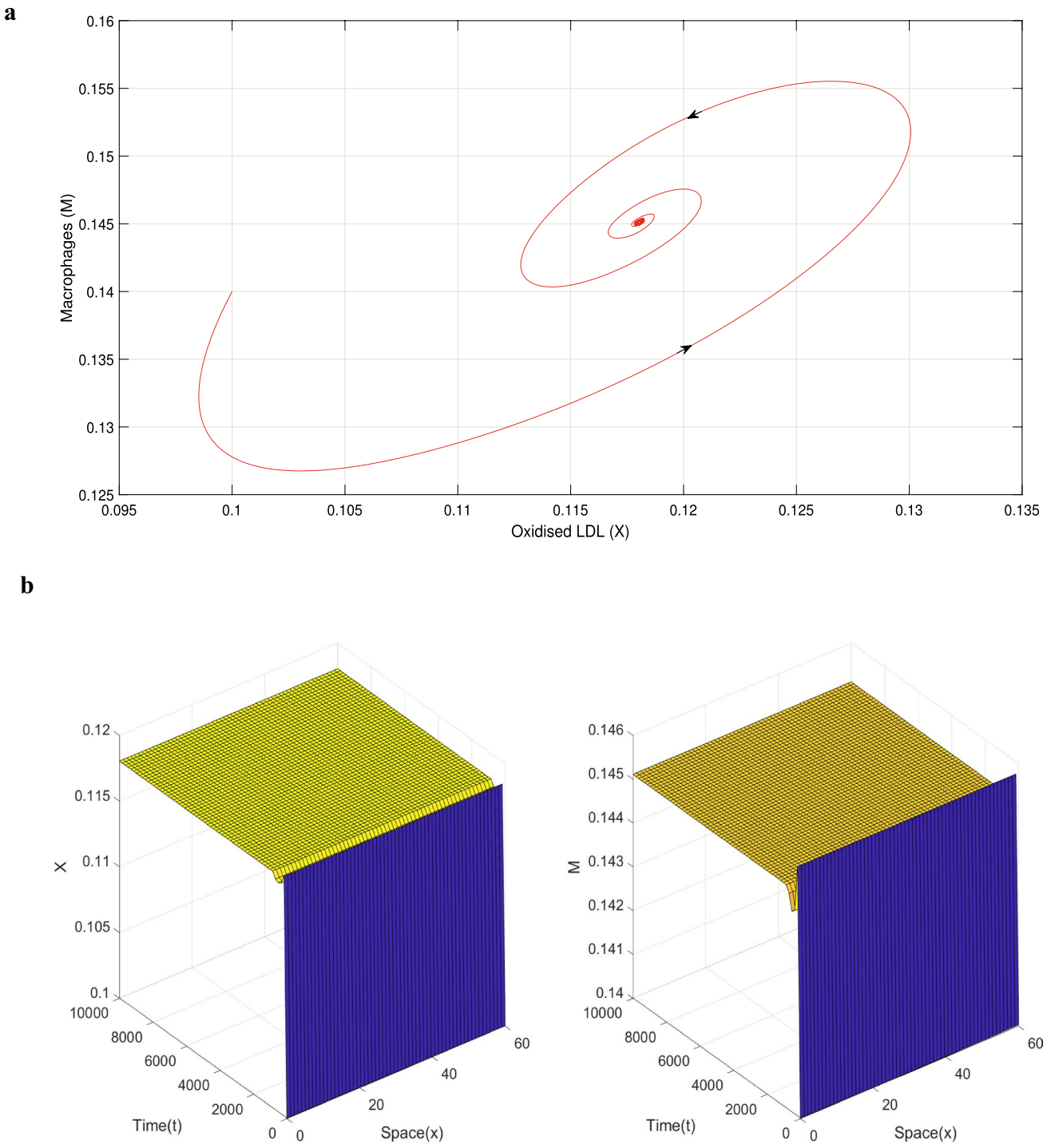

Fig. 2 Global stability around the positive equilibrium point E_2 based on the model parameters provided in Table 1 of **a** the non-spatial system (4.1), (4.2) and **b** the spatial system (3.1), (3.2)

parameters the same as in Table 1 is given in Fig. 4a. The spatial counterpart of this model is exhibiting oscillatory behavior around the positive equilibrium provided in Fig. 4b.

Discussions of the result

Thus, biologically for Fig. 3, one may observe that as the rate of ingestion of macrophages phagocytosing oxidized LDL increases, the plaque deposition process expedites

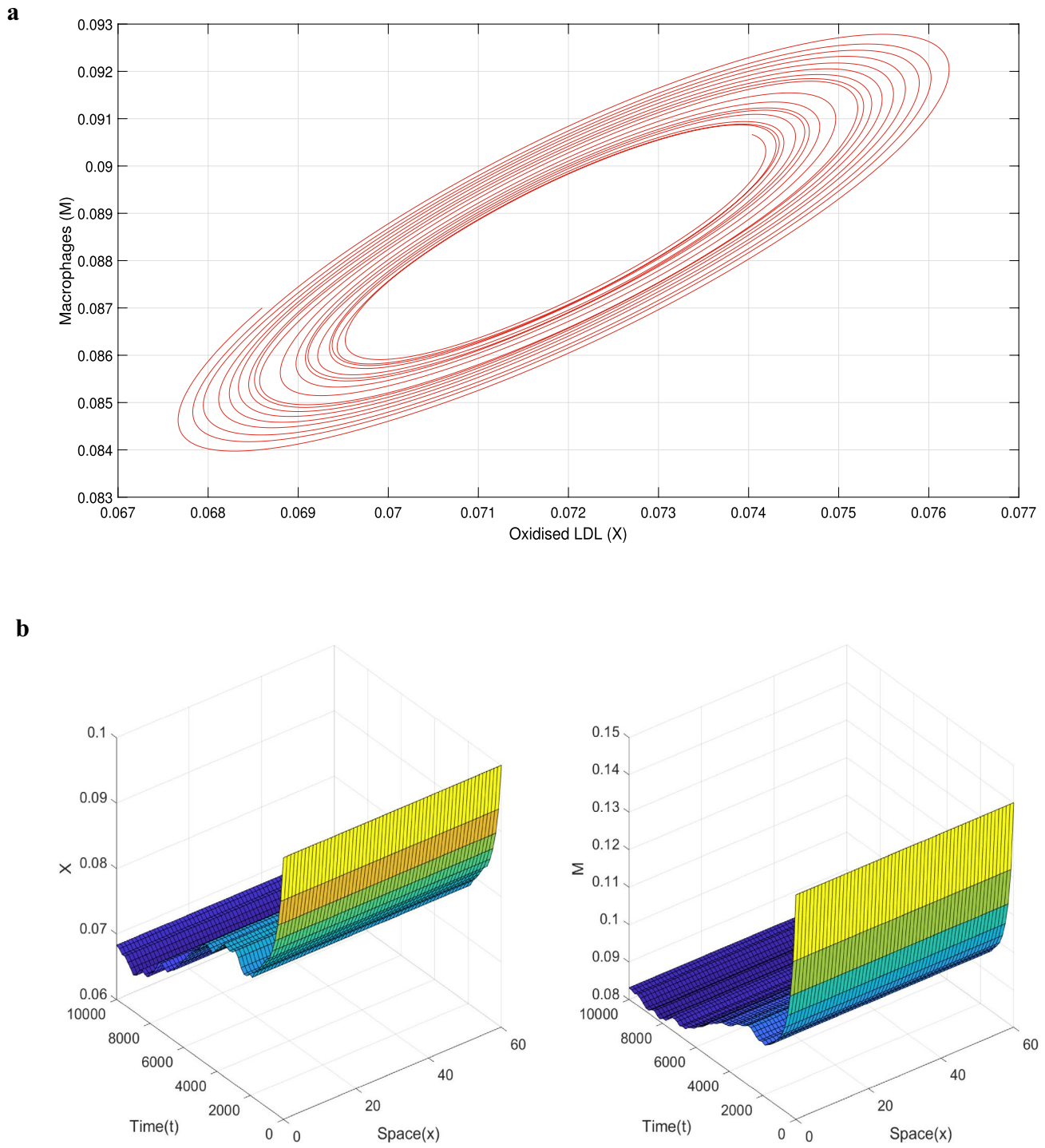

Fig. 3 **a** Phase portrait of the non-spatial model (4.1), (4.2) and **b** Numerical simulation of the spatial system (3.1), (3.2) around E_2 with $D_1 = 1$ and $D_2 = 0.001$ based on $\lambda_1 = 0.233$ and all other model parameter values are same as provided in Table 1

within the intima. Eventually, the plaque volume increases within the intima and it vastly transfigures the vasculature of an individual. From the biological point of view the results obtained in Fig. 4 can be interpreted as, the decrease in the maximum per capita consumption rate of macrophages is the primary reason behind the increase in the plaque volume within the inflammatory region.

The salient features of contemporary research on investigating atherosclerosis formation and evolution depend on certain integral factors. A thorough analysis of the model

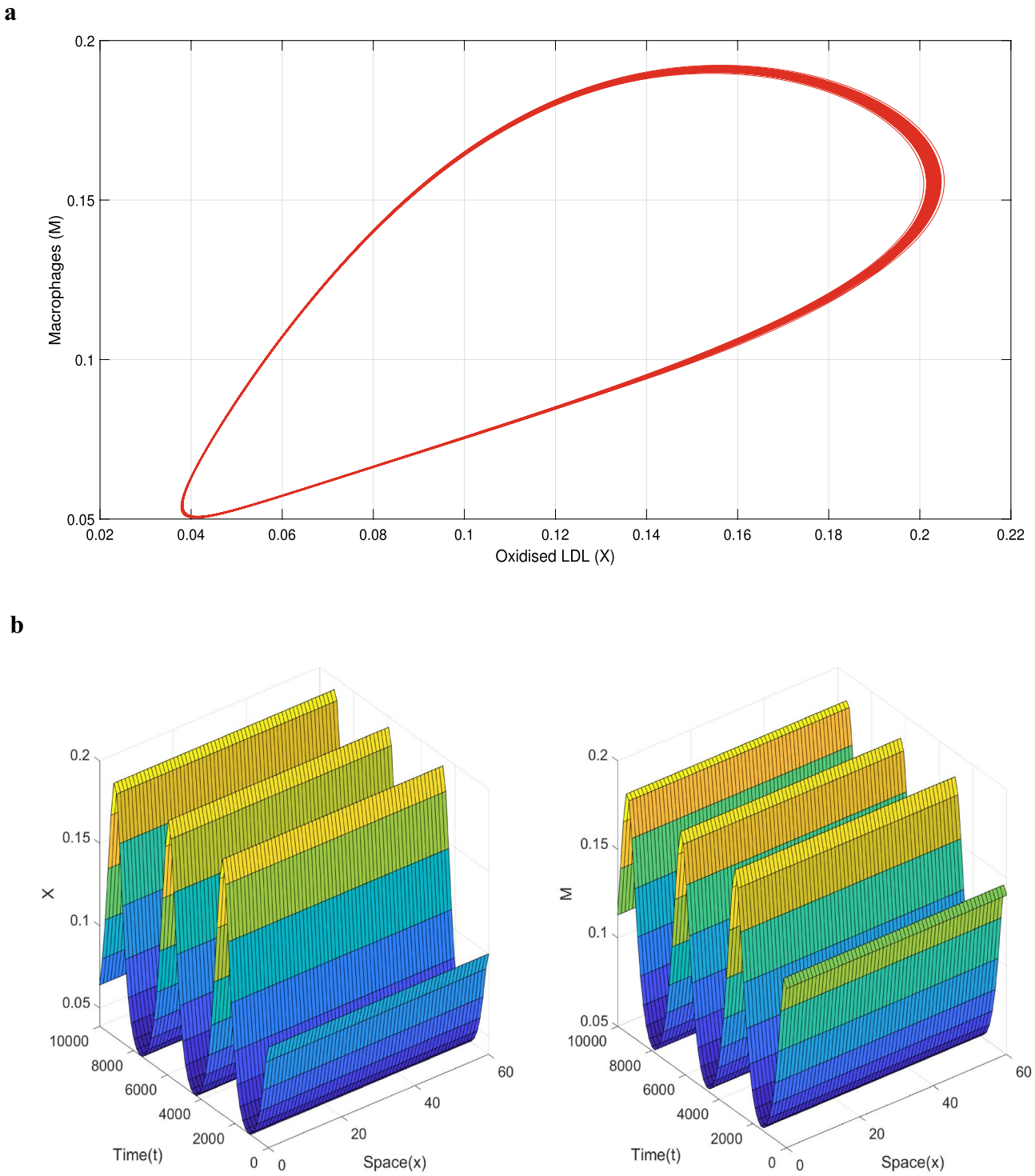

Fig. 4 **a** Phase portrait of the non-spatial model (4.1), (4.2) and **b** numerical simulation of the spatial system (3.1), (3.2) around E_2 with $D_1 = 1$ and $D_2 = 0.001$ based on $a = 0.06$ and all other model parameter values are same as provided in Table 1

reveals two significant model parameters, namely λ_1 and a, where λ_1 is the rate of ingestion of macrophages and a is the rate of per capita consumption rate of macrophages. A slight perturbation in these model parameter values disturbs the stability of the system and hence, bifurcations have been observed with respect to these parameters.

The analytic and numerical results of the model can be biologically interpreted as a small change in clinical therapy

may lead to a vast change in the inflammation process of atherosclerotic plaque formation. The long-term motive of this present work is to provide insight into the significant factors involved in the plaque formation process and to provide a computational platform for further investigation of the disease dynamics.

Concluding remarks

In the present investigation, macrophage phagocytosis, involved in the biochemical process of early stages of atherosclerotic plaque formation, is represented in terms of a reaction–diffusion system of equations. A thorough analysis of both the non-spatial and spatial models shows the stability attributes of the systems under certain conditions. The numerical findings of the non-spatial model provide bifurcation with respect to two significant model parameters namely, λ_1 and a, where λ_1 is the rate of ingestion of macrophages and a is the rate of per capita consumption rate of macrophgaes. The spatial model resembles oscillatory behavior around the positive equilibrium under the bifurcating set of parameter values. The results in this article exhibit the fact that a slight change in the treatment of atherosclerosis may change the outcome significantly.

Acknowledgements All the authors are highly grateful to the anonymous reviewers for their fruitful comments and suggestions.

Declarations

Conflict of interest On behalf of all authors, the corresponding author states that there is no conflict of interest.

References

Abi Younes G, El Khatib N (2022) Math Model Nat Phenom 17:5
Alimohammadi S (2017) Proc Inst Mech Eng Part H J Eng Med 231(5):378
Anlamlert W, Lenbury Y, Bell J (2017) Adv Differ Equ 2017(1):195
Bulelzai MA, Dubbeldam JL (2012) J Theor Biol 297:1
Calvez V, Ebde A, Meunier N, Raoult A (2009) ESAIM Proc (EDP Sci) 28:1–12
Chalmers AD, Cohen A, Bursill CA, Myerscough MR (2015) J Math Biol 71(6–7):1451
Cobbold C, Sherratt J, Maxwell S (2002) Bull Math Biol 64(1):65
Cohen A, Myerscough MR, Thompson RS (2014) Bull Math Biol 76(5):1117
Crowther MA (2005) ASH Educ Program Book 2005(1):436
Friedman A, Hao W (2015) Bull Math Biol 77(5):758
Gijsen FJ, Wentzel JJ, Thury A, Mastik F, Schaar JA, Schuurbiers JC, Slager CJ, van der Giessen WJ, de Feyter PJ, van der Steen AF (2008) Am J Physiol Heart Circ Physiol 295(4):H1608
Hale J (1969) Ordinary differential equations. Pure and applied mathematics. Wiley-Interscience, New York
Hao W, Friedman A (2014) PLoS One 9(3):e90497
Homma S, Hirose N, Ishida H, Ishii T, Araki G et al (2001) STROKE-DALLAS- 32(4):830
Ibragimov A, McNeal C, Ritter L, Walton J (2005) Math Med Biol 22(4):305
Kozusko F, Bourdeau M (2007) Cell Prolif 40(6):824
Libby P, Ridker PM, Maseri A (2002) Circulation 105(9):1135
Malek AM, Alper SL, Izumo S (1999) JAMA 282(21):2035
Marušić M, Vuk-Pavlovic S, Freyer JP et al (1994) Bull Math Biol 56(4):617
Mel'nyk T (2019) Int J Biomath 12(02):1950014
Ougrinovskaia A, Thompson RS, Myerscough MR (2010) Bull Math Biol 72(6):1534
Parton A, McGilligan V, O'kane M, Baldrick FR, Watterson S (2015) Brief Bioinform 17(4):562
Ross R, Glomset J, Harker L (1977) Am J Pathol 86(3):675
Simonetto C, Heier M, Peters A, Kaiser JC, Rospleszcz S (2022) Am J Epidemiol 191 (10):1766 From atherosclerosis to myocardial infarction–a process-oriented model investigating the role of risk factors. 191(10):1766–1775